

# Fatigue Performance of Rib-to-Deck Double-Sided Weld Joint of Orthotropic Steel Deck on Plate Girder Railway Bridges

**Radha Krishna Amritraj**

Department of Civil Engineering, NIT Patna, India  
radhaa.phd19.ce@nitp.ac.in (corresponding author)

**Shambhu Sharan Mishra**

Department of Civil Engineering, NIT Patna, India  
ssmishra@nitp.ac.in

Received: 27 April 2023 | Revised: 10 May 2023 | Accepted: 17 May 2023

Licensed under a CC-BY 4.0 license | Copyright (c) by the authors | DOI: <https://doi.org/10.48084/etasr.5994>

## ABSTRACT

This research work presents the stress behavior of rib-deck weld joints in Orthotropic Steel Deck (OSD) railway bridges. It is essential to determine the most vulnerable load mode of the wheels for fatigue failure of OSD bridges and to improve the fatigue resistance of the welded rib-deck connection. Fatigue performance largely depends on the weld stress. Double-sided welds for rib-deck welds improve fatigue performance. The fatigue behavior of the rib-deck double-sided weld joint has been compared with the single-sided one. This study used Abaqus software to create the global shell model and the solid submodel of the OSD. The results of the structural stress-based finite element analysis indicated that when the center line of the front axle pair of a locomotive coincides with the center line of the midspan of the bridge, the most severe loading condition occurs. The rib near the main girder experiences the maximum structural stress in the weld toe of the rib-deck joint. Moreover, the rib-deck double-sided weld joints have 43.7% less structural stress compared to single-sided weld joints at the root of the weld, and this improves the performance during fatigue of OSDs.

**Keywords-**orthotropic steel deck; rib-to-deck weld joint; double-sided weld; structural stress method; train load

## I. INTRODUCTION

Orthotropic Steel Decks (OSD) are widely used in large-span cable-suspension and -stayed bridges, as they have proven to be a better alternative to the most used steel plate girder railway bridges, from the view of fatigue strength, multi-tracks, high speed, and heavy freight trains. An OSD bridge consists of a structural steel deck plate that is stiffened longitudinally, while transverse stiffeners may be optional. OSDs provide numerous benefits such as low dead weight, substantial load-carrying capacity, and the ability to be built modularly on-site [1-3]. Compared to standard steel plate-girder bridges, the low dead weight features of OSDs translate into considerable steel tonnage savings of up to 50% [4]. In general, OSD bridges are complex structures with many weld connections. Therefore, the strength and life of OSDs are mostly determined by fatigue and fracture of the weld connections and factors such as stress concentrations, the thickness of connecting plates, weld penetration, crack location at the rib-deck weld joints, and position of wheel loads [5-6]. Wheel loads applied directly to the OSD are the predominant factor that leads to fatigue cracks [7-8]. The most vulnerable fatigue cracks in OSD bridges subjected to wheel loads are located in the rib-deck weld

connection [4, 6-10]. Figure 1 shows the rib-deck weld joints of OSDs that are prone to four distinct kinds of fatigue cracks, namely toe-deck (Type 1), root-deck (Type 2), toe-rib (Type 3), and root-weld (Type 4) [4, 10-12].

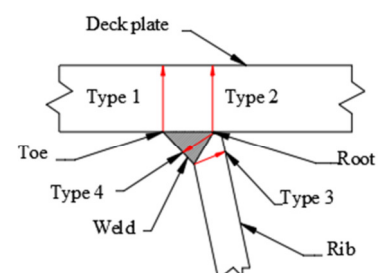


Fig. 1. Rib-deck weld joints.

In [4], the structural stress behavior of the rib-deck weld joints of OSD models was studied numerically, showing that the toe-deck cracking into the deck plate was the dominant among four crack types. In [13], the fatigue behavior of the

most prone to fatigue cracking rib-deck weld joints in OSDs was experimentally investigated, showing that after the beginning of a crack at the weld toe on the bottom surface of the deck plates, it propagates longitudinally till the crack tips reach the deck edges. Then, the fatigue crack spreads through the thickness of the deck plate causing a noticeable fatigue crack to appear on the upper surface of the deck plate.

Several lab tests and numerical investigations have been conducted to improve fatigue performance and study the structural behavior of rib-deck weld joints in OSD bridges. In [12], the fatigue capabilities of single- and double-sided weld joints in OSD rib decks were studied, taking into account both vehicle load and residual stress. The results showed that the most fatigue-critical segment of the rib-deck single-sided weld joint was in the weld root, while in the double-sided weld joint, it was the outer weld toe. Double-sided weld joints in OSDs can minimize the probability of fatigue cracks in the weld root compared to single-sided ones. In [14], an experimental and numerical investigation was conducted on the fatigue behavior of OSD single- and double-side weld joints, concluding that fatigue failure of the single-sided weld joint occurs in the root of the weld, while all the double-sided weld joint samples failed inside the weld toe. In [15], a fatigue test was carried out on single- and double-sided rib-deck weld joints, recommending the latter in OSD weld joints.

In general, most OSDs belong to long-span cable-stayed or suspension bridge box girders. The feasibility of OSDs in short-span bridges still needs to be investigated for improved fatigue life compared to other types of traditional bridges, such as plate girder bridges. In the Indian continent, most railway bridges consist of plate girders with RCC decks. An RCC deck has a high deadweight and requires more time to construct along with a lot of formwork compared to an OSD. Therefore, using OSD on a short-span railway bridge may be a good option in place of an RCC deck. The Indian short-span steel plate girder welded type railway bridges are of lengths 12.2, 18.3, 19.4, and 24.4m. This study investigated the span length of 12.2m, consisting of two main plate girders and an OSD placed over them as a replacement for the RCC deck.

## II. STRUCTURAL STRESS METHOD

The structural stress method based on fracture mechanics and the Paris law was introduced in [14-16] for fatigue life estimation. The structural stress method to predict fatigue performance is insensitive to mesh size and is used to study the fatigue performance of marine pipelines, pressure vessels, and orthotropic steel bridge elements. The internal stress at the toe in the weld along the through-thickness direction is separated into normal stress  $\sigma_x$  and shear stress in the plane  $\tau_{xy}$ . Normal stress is easily subdivided into membrane stress  $\sigma_m$  and bending stress  $\sigma_b$ , based on the forces and moments in equilibria. The vertical shear stress  $\tau_m$  is formed by condensing the in-plane shear stress. However, the impact of the shear stress is usually neglected, considering that it would not significantly affect the growth of fatigue cracks. The addition of membrane stress  $\sigma_m$  and bending stress  $\sigma_b$  defines the structural stress, as given in (1-3) [4, 17]. Abaqus software was used to perform the 3-dimensional Finite Element (FE) analysis on the model shown in Figure 2. An 8-node linear brick solid element C3D8R in

Abaqus was used. To resolve the line forces and line moments corresponding to the middle plane of the deck plate, the forces of nodes (NFORC) from the elements located on either side of the line were entered into the equation of matrix form [4, 9]. Then, the structural stress corresponding to each node along the weld line, shown as a dashed line in Figure 2(b), can be evaluated. The nodal forces are used to obtain membrane stress  $\sigma_m$ , bending stress  $\sigma_b$ , and structural stress  $\sigma_s$  using (1-3).

$$\sigma_m = \frac{1}{t} \sum_{i=1}^n F_i \quad (1)$$

$$\sigma_b = \frac{6}{t^2} \sum_{i=1}^n F_i \times (y_i - t/2) \quad (2)$$

$$\sigma_s = \sigma_m + \sigma_b \quad (3)$$

where  $F_i$  is the nodal force, and  $t$  is the thickness of the plate.

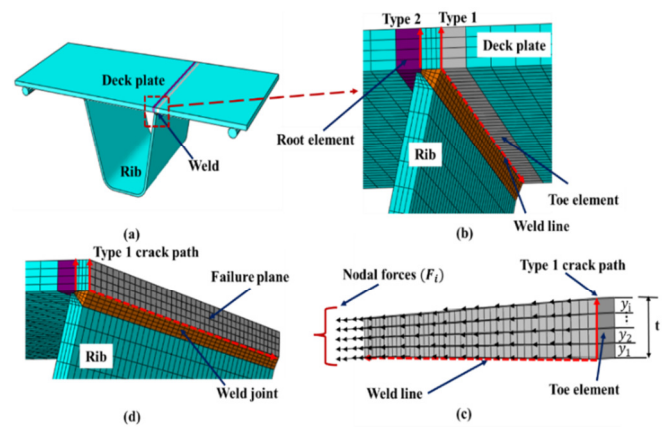


Fig. 2. The 3D solid element model in structural stress calculation.

### A. Master S-N Curve Parameter

In [16], a two-stage crack propagation model was proposed based on an equivalent structural stress parameter obtained using fracture mechanics fundamentals and integrating various data from plate joint fatigue analysis into a narrow-band master S-N curve. With only one curve, the master S-N curve has been used to predict the fatigue characteristics of multiple kinds of weld joints [4, 18]. The impact of stress intensity on the area of concern, the base metal thickness, and several loading modes were recognized in the master S-N curve. The standard deviation of the S-N curve  $\sigma$  was 0.246. Taking into account the impact of the deck plate thickness  $t$ , the stress ratio  $r$  (4), the loading mode parameter  $I(r)^{1/m}$  (5), and the structural stress range  $\Delta\sigma_s$ , the equivalent structural stress range  $\Delta S_s$  can be given by (6) [4, 18]. The parameter  $m$  for the growth of fatigue cracks, used in (5), was taken as 3.6. The fatigue life  $N$  of the deck to rib welded joints can be determined by (7), considering the S-N curve parameters  $h$  and  $C_d$  as shown in Table I [4, 18].

$$r = \frac{|\sigma_b|}{|\sigma_m| + |\sigma_b|} \quad (4)$$

$$I(r)^{\frac{1}{m}} = 0.0011r^6 + 0.0767r^5 - 0.0988r^4 + 0.0946r^3 + 0.0221r^2 + 0.014r + 1.2223 \quad (5)$$

$$\Delta S_s = \frac{\Delta\sigma_s}{t^{(2-m)/2m} \cdot I(r)^{1/m}} \quad (6)$$

$$N = \left( \frac{\Delta S_s}{C_d} \right)^{1/h} \tag{7}$$

TABLE I. MASTER S-N CURVE PARAMETERS

Statistical basis	$C_d$	$h$
Mean	19930.2	-0.32
+2σ (upper 95%)	28626.5	
-2σ (lower 95%)	13875.8	
+3σ (upper 99%)	31796.1	
-3σ (lower 99%)	12492.6	

III. VALIDATION OF THE METHOD

Numerical computations were carried out based on structural stress to investigate the fatigue performance of an OSD, using the loadings, shape, and sizes of [4] to compare results. Two load cases are considered: load case-I and load case-II. The load case-II is critical when studying the fatigue performance of OSDs. The OSD model was 1000 mm long and 400 mm wide. The deck plate, rib thickness, and rib height were 16, 8, and 300 mm. The model was loaded with a 20 kN load, applied eccentrically above the rib-deck junction on the deck surface in a patch area of 250×250 mm. Figure 3 shows geometry, loading, material properties, and boundary conditions [4]. The FE model was discretized using an 8-node C3D8R solid element, available in Abaqus 2019 [19-22].

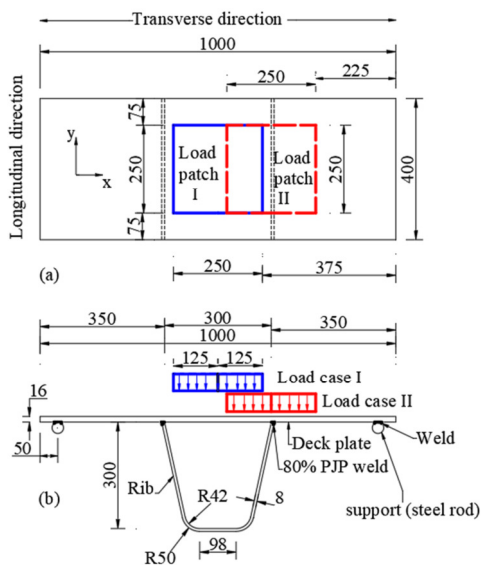


Fig. 3. Dimensional details and loading condition of the model.

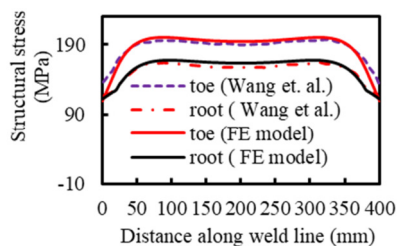


Fig. 4. Structural stress along the weld line at the rib-deck joint.

Figure 4 shows the structural stress results obtained using Abaqus 2019 [21] and Fe-safe 2019 [23]. Structural stresses were obtained for the deck toe (Type 1) and the root (Type 2) cracks. The structural stress values obtained along the weld line of the FE model were close to [4] with only a 3% difference that can be treated as admissible.

IV. FE MODELING OF THE BRIDGE DECK

A FE model was developed to study the structural behavior of rib-deck weld joints of a full-span OSD railway bridge. Stresses on the deck plate at the toe and root of the rib-deck welded joints were calculated using a fracture mechanics-based structural stress method [13-16]. Abaqus [21] and Fe-safe [23] were used to develop the numerical FE model and calculate the structural stress, respectively. Figure 5 shows the geometry of the cross-section of the OSD model and the weld.

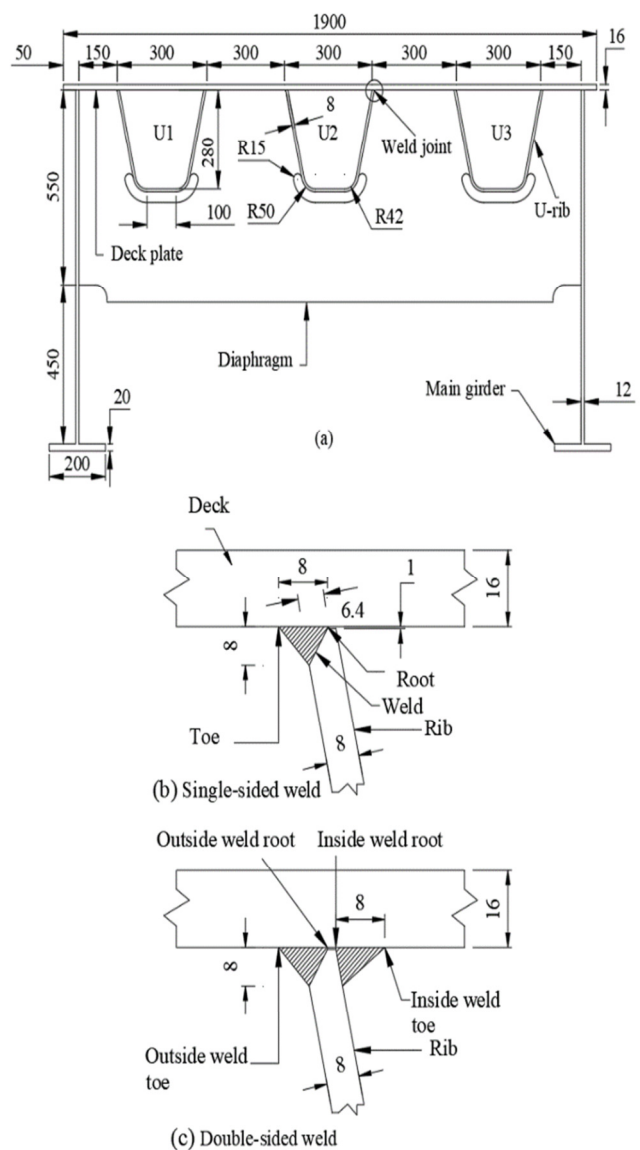


Fig. 5. Dimensional details of (a) the cross-section of the full-span bridge, (b) single-sided weld, and (c) double-sided weld.

The linear elastic material properties of E350 steel, having Young's modulus of elasticity  $2 \times 10^5$  MPa and Poisson's ratio of 0.3, were considered for the model. The global shell model of the considered OSD had 4 diaphragms and 3 U-ribs, as shown in Figure 6(a). The span length and width of the bridge deck were 12.2 and 1.9 m, respectively. A solid sub-model was simulated using the sub-modeling techniques in Abaqus from the full-span model. Boundary conditions of the sub-model were pre-assigned in Abaqus from the nodal displacements of the global model. Figure 6(b) shows the details of the solid sub-model. The lateral and longitudinal lengths of the OSD submodel were kept at 600 and 3600 mm respectively. Shell-to-solid coupling features in Abaqus were used to connect the global model shell element (S4R) and sub-model solid element (C3D8R). The contact surfaces at the weld joint in the solid sub-model were connected by Tie constraints. The number of elements in the global shell model, and the solid sub-model of single- and double-sided welds were 195500, 32640, and 40800, respectively.

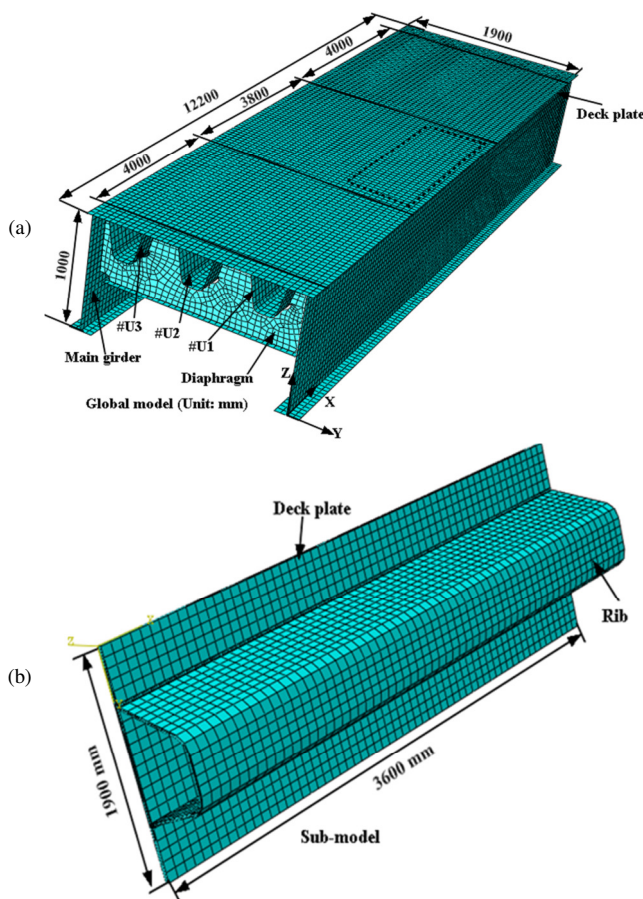


Fig. 6. FE simulation of (a) global shell-model and (b) solid sub-model.

A. Loadings

In this investigation, the axle loads of a 25-ton Indian freight locomotive (train type-7) were considered. According to [24], the length of the sleeper is 2750 mm, the cross-section is 250×250 mm, and the thickness of the ballast layer is 400 mm.

A uniform load intensity of  $0.294 \text{ N/mm}^2$  on the patch area of the deck surface  $450 \times 1900 \text{ mm}^2$  was considered for all models. The longitudinal loading positions were taken as follows: (i) Load Case I (LC-I): with the front axle of the locomotive at the midspan of the bridge (ii) Load Case II (LC-II): with the center line of the pair of the front axles at the midspan of the bridge, and (iii) Load Case III (LC-III): with the center line of the locomotive at the midspan of the bridge. Figure 7 shows the loading conditions.

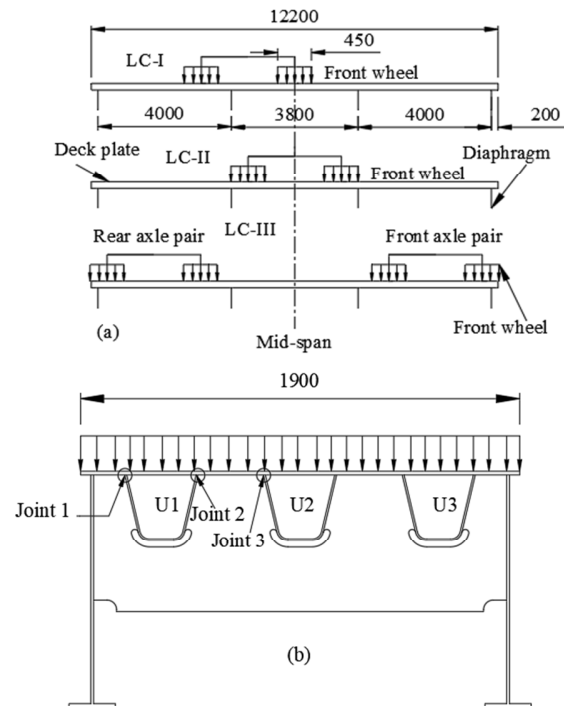


Fig. 7. Loading conditions: (a) longitudinal load positions and (b) constant transverse loading (in mm).

V. RESULTS AND DISCUSSION

This study focused only on the structural stress at the toe and root of the rib-deck weld joints of the considered OSD. Load movement along the bridge was established using a DLOAD user subroutine for Abaqus, developed in FORTRAN. The loading begins when the leading wheels touch the second diaphragm and lasts until the back wheel departs the third diaphragm. Depending on the global shell model, stress distribution curves were obtained along the weld line in the rib-deck weld joints under different loading conditions. The structural stress calculation procedure was described in Section II.

Figure 8 shows the variation in structural stress of three different single-sided rib-deck weld joints of the OSD shown in Figure 5, under the three-axle load positions shown in Figure 7. Figures 8 (a)-(b) show the stress variation of the toe and root at joint 1 for the three loading conditions. Similarly, Figures 8 (c)-(d) show the stress variation of the toe and root for joint 2, and Figures 8 (e)-(f) show the stress variation of the toe and root for joint 3 of the weld along the weld line.

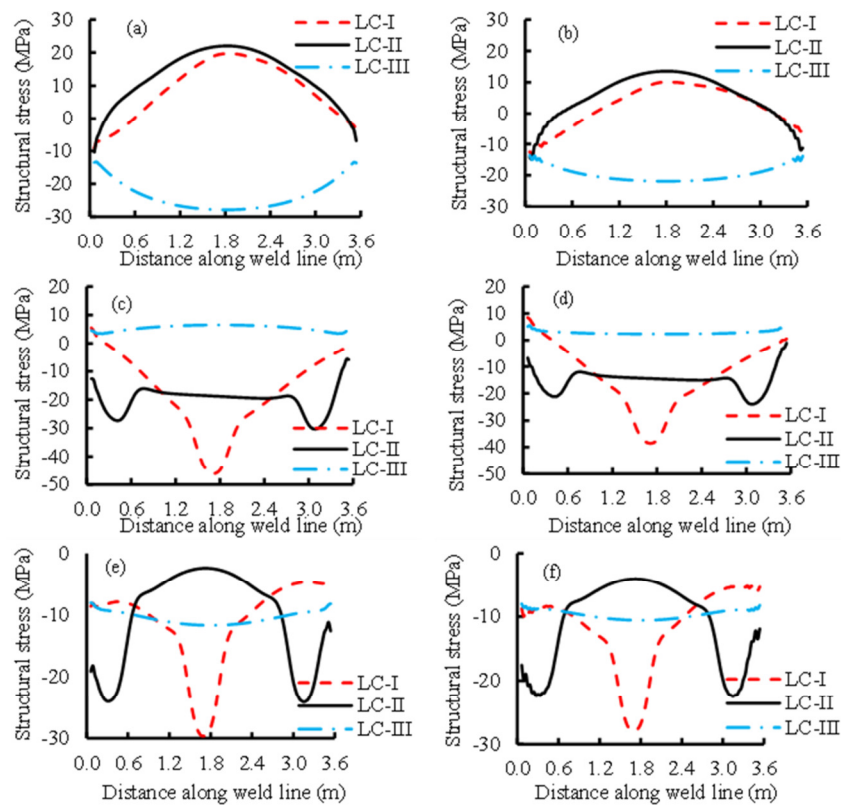


Fig. 8. Stress histogram of single-sided weld joints: (a) Outside weld toe at joint 1, (b) outside weld root at joint 1. (c) outside weld toe at joint 2, (d) outside weld root at joint 2, (e) outside weld toe at joint 3, and (f) outside weld root at joint 3 for different loading positions.

In the single-sided weld, at joint 1, under LC-II, the maximum tensile structural stress arises in the toe and root of the rib-deck weld in each cycle, and it is the most critical loading position from the view of fatigue of the weld details. At joints 2 and 3, under LC-II, the structural stresses were compressive in nature at the toe and root of the weld. Under LC-II loading conditions, the fatigue-prone weld part was the weld toe joint 1 on the rib just near the main girder of the bridge. The fatigue lives of joints 1, 2, and 3 in the case of single-sided welds were also determined using (7). The fatigue life of joints 1, 2, and 3 were  $9.9 \times 10^9$ ,  $3.14 \times 10^{15}$ , and infinite life cycles, respectively. The results for single-sided weld joints showed that only joint 1 experiences maximum stress, while joints 2 and 3 experience negative stresses (compression). Therefore, further stress and fatigue analyses were performed only for joint 1. Figure 9, shows the stress variation for joint 1 in the rib-deck double-sided weld for the outside toe and root under the three loading conditions. In the double-sided weld, at joint 1, under LC-II, the structural stress was maximum at the outside toe of the weld. The fatigue life of joint 1 was also determined in the case of double-sided welds using (7) and was found to be  $1.7 \times 10^{12}$ .

Figure 10 compares the structural stresses for single- and double-sided weld joints. Figure 10 shows that the maximum structural stress at the root of the double-sided rib-deck weld was 7.65 MPa, which is 43.7% less than the maximum stress at the root of the single-sided rib-deck weld under LC-II, which was 13.58 MPa. The stress on the deck plate at the double-

sided weld toe was 22.49 MPa and at the single-sided weld toe was 22.31 MPa, which were approximately the same. A similar trend of results was found in [11-13]. As a result, according to the findings of stress analysis, the OSD's double-sided weld rib-deck joints can significantly reduce the possibility of root-weld fatigue failure.

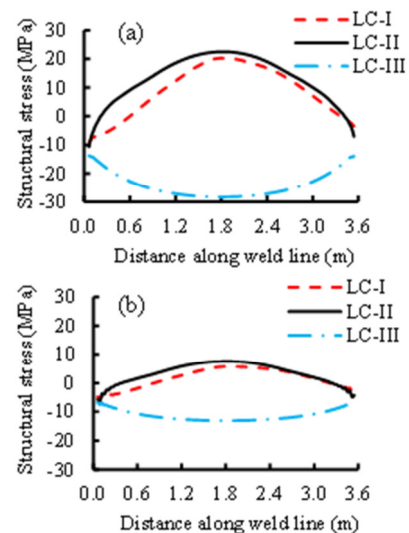


Fig. 9. Stress histogram of double-sided weld at joint 1: (a) Outer weld toe, and (b) outer weld root.

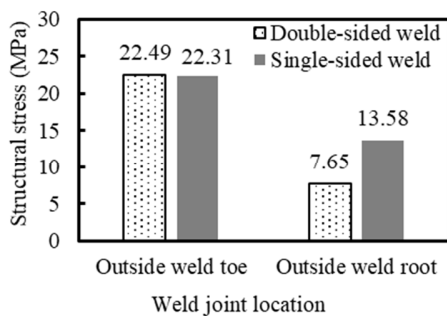


Fig. 10. Comparison of structural stress of weld joints under LC-II.

The novelty of this research work is the intuition of an OSD on one-section steel plate girders to support railway tracks, especially in the region of curves or congestion. A railway short-span bridge consisting of an OSD on a one-section plate girder is a new idea that will carry multiple tracks. The stiffening of the OSD has been proposed with U-ribs having double-sided rib-deck weld joints. Most studies focused on OSDs containing single-sided rib-deck welded joints. This analyzed fatigue stress for double-sided welds for the rib-deck connection. Moreover, a larger loading patch area was considered according to the dispersion allowed in European standards [25-27], in contrast to the smaller patch area of highway bridges.

## VI. CONCLUSIONS

The rib-deck weld joints in an OSD are considered to dictate the fatigue efficiency of the deck. This study carried out an analytical investigation on rib-deck weld joints of a full-span OSD on a steel plate girder bridge. The fatigue performances of rib-deck single- and double-sided weld joints of OSDs for the most severe Indian locomotive axle loading positions were analyzed and compared. The fracture mechanics-based structural stress method was used to evaluate the stresses in the weld joints. The strength and fatigue life of the rib-deck double-sided weld joints were investigated and compared with the single-sided ones. The conclusions are as follows:

- The maximum stress in the root of the double-sided rib-deck weld was observed to be reduced compared to the stress at the corresponding point in the single-sided one. The maximum stress of 7.65 MPa in the root of the double-sided rib-deck weld was 43.7% lower than the maximum stress of 13.58 MPa in the single-sided one. Therefore, there is an improvement in the fatigue performance of OSD.
- No changes in stresses at the toe of the weld connecting the deck plate were found regardless of whether the rib-deck weld is single- or double-sided. The structural stress on the deck plate at the double-sided weld toe was 22.49 MPa and at the single-sided one was 22.31 MPa, which is approximately the same.
- The most severe loading position for single- and double-sided weld joints in OSDs is the LC-II, which is with the center line of the front axle pair of the locomotive at the midspan of the bridge deck. LC-II yields the highest structural stress in the rib weld, which is nearest to the main

girder. This result is in contrast to highway box-girder OSD bridges, where the maximum structural stress occurs in the rib in the middle of the deck.

- The fatigue life of an OSD bridge with double-sided welds for the rib-deck connections is very high compared to one with single-sided rib-deck weld connections. The fatigue life of double- and single-sided welds were  $1.7 \times 10^{12}$  and  $9.9 \times 10^9$  cycles, respectively, in respect of the root of rib-deck weld joints in OSD.

Additional effort is required to conduct an experimental investigation of the fatigue behavior of the rib-deck joints of OSDs. The stress intensity factor [28] may also be calculated at the critical stress locations in the rib-deck weld joints. The limitation of this study is that it was based on a numerical analysis only for the case of train loads.

## REFERENCES

- [1] G. Alencar, A. de Jesus, J. G. S. da Silva, and R. Calçada, "Fatigue cracking of welded railway bridges: A review," *Engineering Failure Analysis*, vol. 104, pp. 154–176, Oct. 2019, <https://doi.org/10.1016/j.engfailanal.2019.05.037>.
- [2] Z. Qing-hua, B. U. Yi-zhi, and L. I. Qiao, "Review on Fatigue Problems of Orthotropic Steel Bridge Deck (in English)," *China Journal of Highway and Transport*, vol. 30, no. 3, pp. 14-31, Mar. 2017.
- [3] S. Zhang, X. Shao, J. Cao, J. Cui, J. Hu, and L. Deng, "Fatigue Performance of a Lightweight Composite Bridge Deck with Open Ribs," *Journal of Bridge Engineering*, vol. 21, no. 7, Jul. 2016, Art. no. 04016039, [https://doi.org/10.1061/\(ASCE\)BE.1943-5592.0000905](https://doi.org/10.1061/(ASCE)BE.1943-5592.0000905).
- [4] P. Wang, X. Pei, P. Dong, and S. Song, "Traction structural stress analysis of fatigue behaviors of rib-to-deck joints in orthotropic bridge deck," *International Journal of Fatigue*, vol. 125, pp. 11–22, Aug. 2019, <https://doi.org/10.1016/j.ijfatigue.2019.03.038>.
- [5] M. S. Pfeil, R. C. Battista, and A. J. R. Mergulhão, "Stress concentration in steel bridge orthotropic decks," *Journal of Constructional Steel Research*, vol. 61, no. 8, pp. 1172–1184, Aug. 2005, <https://doi.org/10.1016/j.jcsr.2005.02.006>.
- [6] S. Ya, K. Yamada, and T. Ishikawa, "Fatigue Evaluation of Rib-to-Deck Welded Joints of Orthotropic Steel Bridge Deck," *Journal of Bridge Engineering*, vol. 16, no. 4, pp. 492–499, Jul. 2011, [https://doi.org/10.1061/\(ASCE\)BE.1943-5592.0000181](https://doi.org/10.1061/(ASCE)BE.1943-5592.0000181).
- [7] Z.-G. Xiao, K. Yamada, S. Ya, and X.-L. Zhao, "Stress analyses and fatigue evaluation of rib-to-deck joints in steel orthotropic decks," *International Journal of Fatigue*, vol. 30, no. 8, pp. 1387–1397, Aug. 2008, <https://doi.org/10.1016/j.ijfatigue.2007.10.008>.
- [8] S. Zengah, A. Aid, and M. Benguediab, "Comparative Study of Fatigue Damage Models Using Different Number of Classes Combined with the Rainflow Method," *Engineering, Technology & Applied Science Research*, vol. 3, no. 3, pp. 446–451, Jun. 2013, <https://doi.org/10.48084/etasr.325>.
- [9] J. Li, Q. Zhang, Y. Bao, J. Zhu, L. Chen, and Y. Bu, "An equivalent structural stress-based fatigue evaluation framework for rib-to-deck welded joints in orthotropic steel deck," *Engineering Structures*, vol. 196, Oct. 2019, Art. no. 109304, <https://doi.org/10.1016/j.engstruct.2019.109304>.
- [10] R. Wolchuk, "Lessons from Weld Cracks in Orthotropic Decks on Three European Bridges," *Journal of Structural Engineering*, vol. 116, no. 1, pp. 75–84, Jan. 1990, [https://doi.org/10.1061/\(ASCE\)0733-9445\(1990\)116:1\(75\)](https://doi.org/10.1061/(ASCE)0733-9445(1990)116:1(75)).
- [11] F. Jiang, Z. Fu, B. Ji, and L. Wan, "Fatigue life evaluation of deck to U-rib welds in orthotropic steel deck integrating weldment size effects on welding residual stress," *Engineering Failure Analysis*, vol. 124, Jun. 2021, Art. no. 105359, <https://doi.org/10.1016/j.engfailanal.2021.105359>.

- [12] Y. Liu, F. Chen, N. Lu, L. Wang, and B. Wang, "Fatigue performance of rib-to-deck double-side welded joints in orthotropic steel decks," *Engineering Failure Analysis*, vol. 105, pp. 127–142, Nov. 2019, <https://doi.org/10.1016/j.engfailanal.2019.07.015>.
- [13] B. Cheng, X. Ye, X. Cao, D. D. Mbako, and Y. Cao, "Experimental study on fatigue failure of rib-to-deck welded connections in orthotropic steel bridge decks," *International Journal of Fatigue*, vol. 103, pp. 157–167, Oct. 2017, <https://doi.org/10.1016/j.ijfatigue.2017.05.021>.
- [14] H. Yang, P. Wang, H. Qian, S. Niu, and P. Dong, "An experimental investigation into fatigue behaviors of single- and double-sided U rib welds in orthotropic bridge decks," *International Journal of Fatigue*, vol. 159, Jun. 2022, Art. no. 106827, <https://doi.org/10.1016/j.ijfatigue.2022.106827>.
- [15] C. Fan, L. Da, K. Wang, S. Song, and H. Chen, "Fatigue Tests and Failure Mechanism of Rib-to-Deck Welded Joints in Steel Bridge," *Sustainability*, vol. 15, no. 3, Jan. 2023, Art. no. 2108, <https://doi.org/10.3390/su15032108>.
- [16] P. Dong, M. Prager, and D. Osage, "The Design Master S-N Curve in ASME Div 2 Rewrite and its Validations," *Welding in the World*, vol. 51, no. 5, pp. 53–63, May 2007, <https://doi.org/10.1007/BF03266573>.
- [17] P. Dong, "A Robust Structural Stress Method for Fatigue Analysis of Offshore/Marine Structures," *Journal of Offshore Mechanics and Arctic Engineering*, vol. 127, no. 1, pp. 68–74, Mar. 2005, <https://doi.org/10.1115/1.1854698>.
- [18] P. Dong, "A structural stress definition and numerical implementation for fatigue analysis of welded joints," *International Journal of Fatigue*, vol. 23, no. 10, pp. 865–876, Nov. 2001, [https://doi.org/10.1016/S0142-1123\(01\)00055-X](https://doi.org/10.1016/S0142-1123(01)00055-X).
- [19] H. Yang, P. Wang, H. Qian, and P. Dong, "Fatigue Performance of Different Rib-To-Deck Connections Using Traction Structural Stress Method," *Applied Sciences*, vol. 10, no. 4, Jan. 2020, Art. no. 1239, <https://doi.org/10.3390/app10041239>.
- [20] T. Marin and G. Nicoletto, "Fatigue design of welded joints using the finite element method and the 2007 ASME Div. 2 Master curve," *Frattura ed Integrità Strutturale*, vol. 3, no. 9, pp. 76–84, 2009, <https://doi.org/10.3221/IGF-ESIS.09.08>.
- [21] "Abaqus Theory Manual," Abaqus Software s.a.r.l., Paris, France, 2014.
- [22] Y. Almoosi, J. McConnell, and N. Oukaili, "Evaluation of the Variation in Dynamic Load Factor Throughout a Highly Skewed Steel I-Girder Bridge," *Engineering, Technology & Applied Science Research*, vol. 11, no. 3, pp. 7079–7087, Jun. 2021, <https://doi.org/10.48084/etasr.4106>.
- [23] "SIMULIA fe-safe Durability Analysis Software for Finite Element Models." Trimech, 2019. Available: <https://enterprise.trimech.com/simulia/fe-safe/>.
- [24] RDSO, "Indian Railway Standard Code of Practice for the Design of Steel or Wrought Iron Bridges carrying Rail, Road or Pedestrian Traffic," Research Design and Standards Organisation, Lucknow, India, 2003.
- [25] "EN 1991-2:2003 Eurocode 1. Actions on structures - Part 2: Traffic loads on bridges," European Committee for Standardization, Brussels, Belgium, European Standard, 2003.
- [26] "EN 1993-1-9:2005 Eurocode 3: Design of steel structures - Part 1-9: Fatigue," European Committee for Standardization, Brussels, Belgium, European Standard, 2005.
- [27] "EN 1993-2:2006 Eurocode 3: Design of steel structures - Part 2: Steel bridges," European Committee for Standardization, Brussels, Belgium, European Standard, 2006.
- [28] Y. Kambouz, M. Benguediab, and B. Bouchouicha, "Numerical Analysis of Crack Progress in Different Areas of a Friction Stir Welded Bead for an 5251 H14 Aluminum Alloy Specimen," *Engineering, Technology & Applied Science Research*, vol. 4, no. 1, pp. 581–586, Feb. 2014, <https://doi.org/10.48084/etasr.381>.